

Integration of organic light-emitting diode and organic transistor via a tandem structure

Chih-Wei Chu, Chieh-Wei Chen, Sheng-Han Li, Elbert Hsing-En Wu, and Yang Yang^{a)}
Department of Materials Science and Engineering, University of California, Los Angeles, Los Angeles, California 90095

(Received 20 December 2004; accepted 22 April 2005; published online 14 June 2005)

A high-performance organic active matrix pixel was fabricated by using a metal oxide (V_2O_5) coupling layer that effectively integrates an organic light-emitting diode (OLED) on top of an organic field-effect transistor (OFET). The field-effect mobility of the OFET approached $0.5 \text{ cm}^2 \text{ V}^{-1} \text{ s}^{-1}$ and the ON/OFF current ratio was $>10^3$. The brightness of the OLED was on the order of 2000 cd/m^2 , with an efficiency above 3.3 cd/A . The present work describes in detail a methodology for sizing and stacking an OFET in bottom-emitting active matrix pixel circuits. The confinement of pixel dimension ensures the uniformity of light emission. The material for coupling layer can be tailored to achieve maximum device efficiency. A unique active matrix pixel circuit is proposed that renders both the OFET and OLED their individual performance after integration.
© 2005 American Institute of Physics. [DOI: 10.1063/1.1941461]

Since the finding of electroluminescence from vacuum-deposited organic film reported by Tang *et al.*¹ in 1987, there has been tremendous effort, both academically and commercially, towards the development of organic electronics. Among them, the organic light-emitting diode (OLED) has been studied most extensively due to its low fabrication cost and mechanical flexibility.²⁻⁵ As a result, it has become possible to fabricate low-cost flexible displays. Recent progress in the OLED has focused on maximizing the electroluminescence (EL) efficiency. The current state-of-the-art figure is approximately 10^5 cd/m^2 .^{6,7} There are two generally adopted addressing schemes to integrate a lighting device into electronic display. First is passive matrix addressing, where for N number of emitting rows, each row is addressed with $1/N$ of the frame time. Since the response time of each emitter is limited, PM scheme is limited to low content display.⁶ In addition, the high leakage current in nonselected pixels and high voltage drop across the intersection electrodes exacerbate the already deficient lifetime of OLED at such high luminance. Fortunately, the lifetime issue can be resolved using the active matrix (AM) scheme in which a thin-film transistor combined with a capacitor, is applied to function as a switch for each OLED.⁸⁻¹⁰ In turn, the AM scheme not only allows high information content display, but also provides low power consumption, high brightness, and improved gray scale capability. Generally, amorphous or polycrystalline silicon¹¹ have been the choice of material for the thin-film transistor in order to achieve a high filling factor and low stress direction for light emission. However, silicon transistors are incompatible with plastic substrates due to their complicated processing at high temperatures. On the other hand, organic thin film transistors (OTFTs) have the advantages of light weight, simple fabrication process, and compatible integration with flexible plastic substrates.^{12,13} To exploit the possibility of applying AM schemes on plastic substrates, we use organic transistors in our smart pixel devices.

There have been many attempts to fabricate AM pixels using all-polymer^{14,15} and all-organic^{16,17} materials. Siringhaus *et al.*¹⁴ reported a polymer field effect transistor with ON/OFF current ratio and field-effect mobility as high as 10^6 and $0.05 \text{ cm}^2/\text{V s}$, respectively, in the AM pixel. However, the external quantum efficiency of the individual polymer light-emitting diodes in such scheme was reduced by two orders of magnitude due to unbalanced carrier injection at the source and drain electrodes of the field-effect transistor (FET). By replacing the emitting unit with OLED, Dodabalapur *et al.*¹⁶ were able to increase the external quantum efficiency to nearly 0.45%. Recently, an OLED driven by pentacene-based FET was reported by Kitamura *et al.*¹⁷ Their combined device has individual field-effect mobility of $0.1 \text{ cm}^2/\text{V s}$, ON/OFF ratios of 10^3 , and luminous efficiency of 17 cd/A . However, this approach still required deposition of SiO_2 layer to define the emission area.

In conventional design rules, a current density of 10 mA/cm^2 supplied by the FET must obtain a luminance greater than 100 cd/m^2 in order to be sufficient for indoor viewing.¹⁸ In this letter, we introduce a coupling layer connecting the OLED and the organic FET (OFET) which allowed such luminance in organic AM device. This coupling layer serves two purposes. The first is to control the work function of the adjacent electrode and second is to improve the interface between the organic layer and the electrode, which in turn controls charge injection. This is the missing factor in the attempts to integrate the two devices,¹⁴ which results in the reduction of the quantum efficiency of the OLED and the field-effect mobility of the FET. In addition, we describe an effective integration structure of an OLED and a pentacene-based FET with polymer as the insulator. The structure significantly increases the filling factor and simplifies the metal wiring in the AM addressing scheme. V_2O_5 was proposed to replace indium tin oxide (ITO) as hole injector of charge generation layer in tandem-EL devices.¹⁹ With the insertion of a V_2O_5 coupling layer between OFET and OLED that modifies the injection barrier between the drain and the organic layer, we were able to obtain a comparable current density at a lower operating voltage of the

^{a)}Electronic mail: yangy@ucla.edu

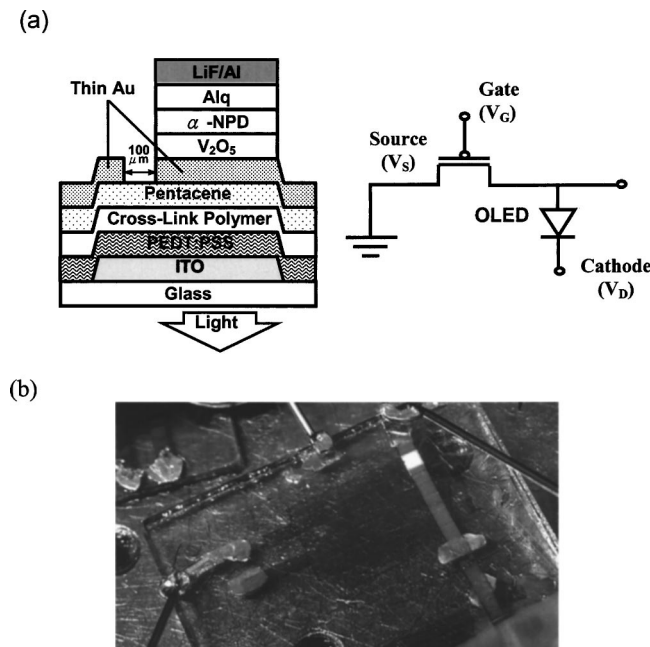


FIG. 1. (a) Schematic of the cross section of the integrated OTFT and OLED and the equivalent circuit diagram. The combined device is the basic constituent of a full active matrix pixel. (b) Photograph of an operating device.

OLED. The electrical characteristics of AM pixel with and without the coupling layer are compared. Our effective integration scheme illustrates the possibility of simple fabrication in using organic molecules for multilayer structured pixels.

The integrated devices were fabricated by first making OFETs using ITO patterned glass substrate as the gate electrode. In order to decrease the leakage from gate to source and drain, a 30 nm thick 3,4-polyethylenedioxythiophene-polystyrenesulfonate (PEDOT:PSS) was subsequently spin coated onto the ITO surface. The PEDOT:PSS layer also serves to smooth the originally rough ITO surface.²⁰ The materials pentacene, poly-4-vinylphenol (PVP, $M_w=20\,000$), poly(melamine-co-formaldehyde) methylated ($M_n=511$), polyoxyethylene(12) tridecyl ether (PEO12), and propylene glycol monomethyl ether acetate (PGMEA) were purchased from Sigma-Aldrich. α -NPD (N,N'-diphenyl-N,N'-bis(1-naphthyl)-1,1'-biphenyl-4,4'-diamine) and Alq₃ [Tris(8-hydroxyquinolato)aluminum] were obtained from e-Ray Optoelectronics Technology. The insulating layer was prepared by dissolving PVP (11%) and poly(melamine-co-formaldehyde) methylated (4%) in PGMEA. The solution was then spin coated onto the PEDOT:PSS/ITO substrates and prebaked at 100 °C for 5 min. Followed by secondary baking at 200 °C for 15 min, this polymer layer started to form a crosslinked structure. To improve the surface roughness of pentacene film, PEO12 (0.05%) was first dissolved in 2-ethoxyethanol, then spin coated on the crosslink polymer. Pentacene was then thermally deposited as the semiconducting layer. The gold source and drain electrodes (10 nm) were then evaporated through a shadow mask. To fabricate the OLED, a 12 nm thick V₂O₅ was first evaporated onto the OTFT. An α -NPD layer and an Alq₃ layer with thicknesses of 40 and 60 nm, respectively, were successively evaporated to form the OLED structure. Lastly, the integrated device was completed by the thermal evaporation of LiF and Al

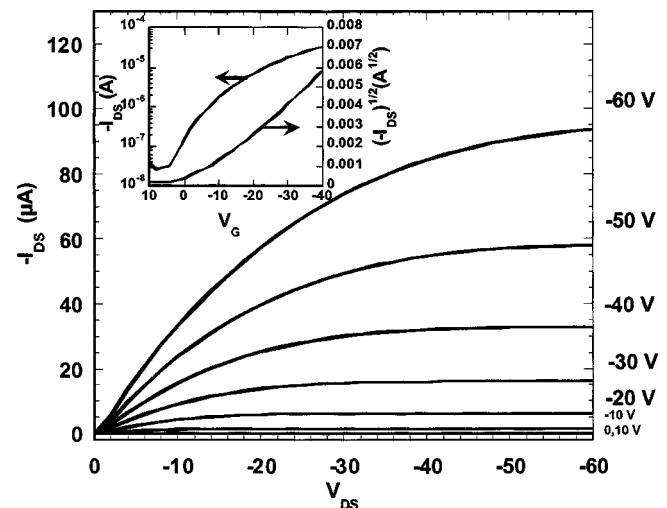


FIG. 2. Output characteristics of the pentacene TFT for different gate-source voltage. The inset shows the $I_D-(I_D)^{1/2}-V_G$ plots at $V_{DS}=-40$ V.

electrodes with a thickness of 0.5 and 80 nm, respectively. The electrical and optical measurements were performed in a nitrogen atmosphere at the room temperature using a HP 4155B semiconductor analyzer and PR-650 SpectraScan spectrophotometer.

Figure 1(a) shows the cross section of the integrated device, which is comprised of an OLED lying on top of a pentacene-based FET. The OLED has a bottom-emitting configuration with a semitransparent metal anode. A photograph of the operating device is shown in Fig. 1(b). The light-emitting area of the OLED was 1 mm², and the channel length (L) and width (W) of pentacene transistor were 100 and 6000 μ m, respectively. The typical output characteristic of the individual OFET is shown in Fig. 2. It showed a saturation region with ON/OFF current ratio of approximately 10³. Based on the $(I_{SD}^{sat})^{1/2}$ versus V_G characteristic, we were able to obtain a field-effect mobility of 0.18 cm²/V s and a threshold voltage of -4.6 V in the saturation region at $V_{DS}=-40$ V. The overall performance of the pentacene-based FETs was comparable to the inorganic amorphous Si:H

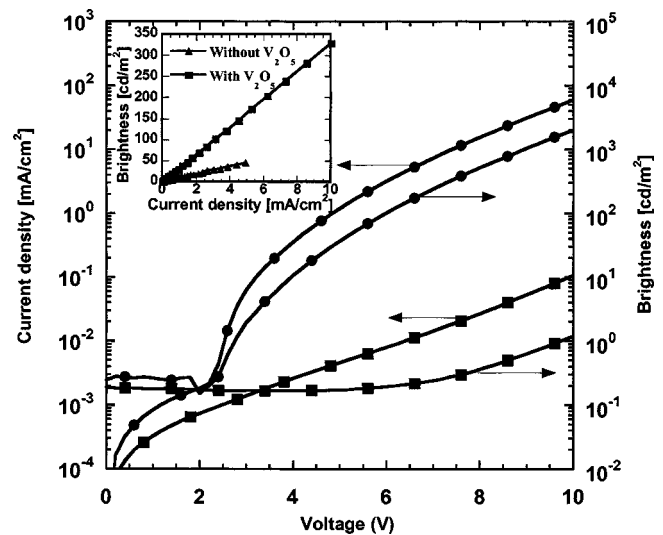


FIG. 3. Brightness-current-voltage characteristics of the EL device (●) with and (■) without V₂O₅. The inset shows the brightness as a function of forward bias current.

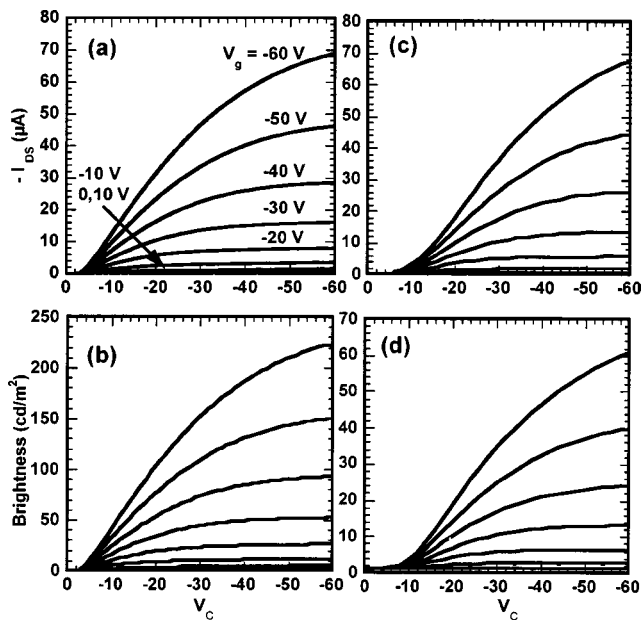


FIG. 4. Output characteristic of an integrated emissive pixel: (a) and (b) with V_2O_5 . (c) and (d) without V_2O_5 .

FETs, and the performance was not degraded even when the OFET was stacked with an OLED device.

The brightness-current density-voltage (B - I - V) and the corresponding B - I characteristics of the individual OLED devices integrated to OFET, both with and without the V_2O_5 coupling layer, are shown in Fig. 3. From the I - V characteristics, the diode shows a clear turn-on voltage at 2.2 V when the V_2O_5 coupling layer is present, and showed no clear turn-on voltage when the V_2O_5 layer was removed. In addition, the current density and the brightness increased dramatically with the presence of the V_2O_5 layer. This suggests that the coupling layer reduced the hole injection barrier at the metal/organic interface and created a more homogeneous adhesion between the hole transporting layer and the anode. Due to lifetime issues, an EL device should operate at a low current density without compromising its brightness. At a constant current density of 5 mA/cm², the device with V_2O_5 coupling layer had a luminance of 162 cd/m², which corresponds to a luminance efficiency of 3.3 cd/A. In contrast, the device without V_2O_5 layer shows the luminance efficiency of only 0.9 cd/A at a similar current density. The improvement in both brightness and efficiency of the integrated devices can be attributed to more balanced injection of holes and electrons.

The cathode voltage V_C , versus OLED current and brightness characteristic curves of the integrated device are shown in Fig. 4. The integrated device exhibited the characteristics of a unipolar FET with good saturation behavior as shown in Figs. 4(a) and 4(c). At small voltage, the output characteristic of the device showed an injection barrier for holes from the higher unoccupied molecular orbital levels of Au to α -NPD. A more balanced injection of holes and electrons was achieved after inserting the coupling layer. The brightness characteristics of the devices are shown in Figs. 4(b) and 4(d). The light emission associated with the electrical output characteristic increased with increasing gate-

source voltage. This is attributed to the effect of the gate-source voltage modulating the carrier density in the channel. Accordingly, by applying a negative voltage between cathode and source, the magnitude of holes and electrons injected into the emissive layer can be controlled by the carrier density. The emission area is confined by the drain electrode with uniformity of light emission. By supplying a current density of 5 mA/cm² with $V_g = -50$ V, LED illuminated with a brightness on the order of 162 cd/m² as shown in Fig. 4(b), which is sufficient for indoor viewing (typically 100 cd/m²). Our results are promising and clearly demonstrate the viability of our technological approach to prepare a multilayer device. With this fabrication technology it is possible to achieve large-area, high-resolution displays using all organic material on plastic substrate.

This technology can be used in integration of other similar organic devices. This idea introduces various possibilities for tuning the electrical properties of the integrated devices. The natural compatibility of the functional material between LED and FET will be further discussed elsewhere.

The authors would like to thank Dr. H. M. Liem for discussion and his valuable help in this work. The financial support is from the Air Force Office of Scientific Research (program manager Dr. Charles Lee, grant No. F49620-03-1-0101). C.-W. Chen gratefully acknowledges the financial support from MediaTek.

¹C. W. Tang and S. Van Slyke, Appl. Phys. Lett. **51**, 913 (1987).

²Y. Kijima, N. Asai, N. Kishii, and S. Tamura, IEEE Trans. Electron Devices **44**, 1222 (1997).

³T. Tohma, Int. Display Research conference (IDRC) Dig. Tech. Papers, 1997, Paper FI.1.

⁴G. Gustafsson, Y. Cao, G. M. Treacy, F. Klavetter, N. Colaneri, and A. J. Heeger, Nature (London) **357**, 477 (1992).

⁵G. Gu, P. E. Burrows, S. Venkatesh, and S. R. Forrest, Opt. Lett. **22**, 172 (1997).

⁶G. Gu and S. R. Forrest, IEEE J. Sel. Top. Quantum Electron. **4**, 83 (1998).

⁷E. I. Haskal, M. Buechel, J. F. Dijkstra, P. C. Duineveld, E. A. Meulenkamp, C. A. H. A. Mutsaers, A. Sempel, P. Snijder, S. I. E. Vulto, P. van de Weijer, and S. H. P. M. de Winter, SID 2002, p. 776.

⁸A. Hunze, M. Scheffel, J. Birnstock, J. Blässing, A. Kanitz, W. Rogler, G. Wittmann, A. Winnacker, S. Rajoelson, and H. Hartmann, SID 2002, p. 1186.

⁹Y. Sakaguchi, H. Tada, T. Tanaka, E. Kitazume, K. Mori, S. Kawashima, and J. Suzuki, SID 2002, p. 1182.

¹⁰S. Xiong, B. Guo, C. Wu, Y. Chen, Y. Hao, Z. Zhou, and H. Yang, SID 2002, p. 1174.

¹¹H. H. Kim, T. M. Miller, E. H. Westerwick, Y. O. Kim, E. W. Kwock, M. D. Morris, and M. Cerullo, J. Lightwave Technol. **12**, 2107 (1994).

¹²L. Ma and Y. Yang, Appl. Phys. Lett. **85**, 5084 (2004).

¹³C. D. Sheraw, L. Zhou, J. R. Huang, D. J. Gundlach, and T. N. Jackson, Appl. Phys. Lett. **80**, 1088 (2002).

¹⁴H. Sirringhaus, N. Tessler, and R. Friend, Science **280**, 1741 (1998).

¹⁵Z. L. Li, S. C. Yang, H. F. Meng, and Y. S. Chen, Appl. Phys. Lett. **84**, 3558 (2004).

¹⁶A. Dodabalapur, Z. Bao, A. Makhija, J. K. Laquindanum, V. R. Raju, Y. Feng, H. E. Katz, and J. Rogers, Appl. Phys. Lett. **73**, 142 (1998).

¹⁷M. Kitamura, T. Imada, and Y. Arakawa, Appl. Phys. Lett. **83**, 3410 (2003).

¹⁸D. Braun and A. J. Heeger, Appl. Phys. Lett. **58**, 1982 (1991).

¹⁹J. Kido, T. Matsumoto, T. Nakada, J. Endo, K. Mori, N. Kawamura, A. Yoko, SID 2003, p. 964.

²⁰F. C. Chen, C. W. Chu, J. He, and Y. Yang, Appl. Phys. Lett. **85**, 3295 (2004).